SUPERCRITICAL CONVECTIVE FLOWS OF MELT WATER IN AN OPEN HORIZONTAL RECTANGULAR CAVITY WITH A PRESCRIBED VERTICAL HEAT FLUX

V.A. Sharifulin[1], T.P. Liubimova[2]

[1]Perm National Research Polytechnic University, Perm, Russian Federation
[2]Institute of Continuous Media Mechanics UB RAS, Perm, Russian Federation

The influence of the intensity of heating, expressed by the Grashof number, on supercritical regimes of thermal convection of melt water in a horizontal rectangular cavity with an aspect ratio of two is investigated. The thermal insulation conditions are satisfied on the lateral solid boundaries, and a constant vertical heat flux is set on the lower solid and upper free, horizontal and non-deformable, edges. Provided that the average temperature over the cavity is close to the density inversion temperature of water in the cavity, a state of mechanical equilibrium is possible, when a stably stratified layer is located on top of an unstable stratified layer. For two cases of the position of the horizontal boundary between these layers, the structure of stationary planar supercritical thermal convection is considered. The calculations were carried out by the finite-difference method on a square grid with 128 nodes along the horizontal coordinate and 64 along the vertical one. Calculations have shown that, with an equal thickness of unstable and stably stratified layers, supercritical convection in the region up to about six supercriticalities has a two-cell structure in the horizontal direction with two (large at the bottom and weaker at the top) vortices in each of the cells. With an increase in supercriticality, this two-cell structure turns into a four-cell structure in a hysteresis manner. For the case when the thickness of the stably stratified layer is three times less than the thickness of the unstable stratified layer, the supercritical convective flow has the general form of a single-vortex cell elongated horizontally. With an increase in the Grashof number up to about a hundredfold supercriticality, it remains generally single-vortex and does not experience bifurcations.

Key words: hysteresis and bifurcations, thermal density inversion, constant heat flux, finite difference method

1. Introduction

The onset of convection in a horizontal liquid layer heated from below with temperature inversion of density and free non-deformable boundaries was studied in [1]. The case of isothermal boundaries is considered, and a hard excitation of convection is found. The author of the work, G. Veronis, suggested approximating the non-linear dependence of water density on temperature by a simple quadratic formula, which in modern notation looks like:

$$\rho = \rho_m \left(1 - \alpha_2 \left|T - T_i\right|^2\right), \tag{1}$$

where ρ_m is the density at $T = T_i$, T_i is temperature of density inversion, $\alpha_2 = 0{,}8 \cdot 10^{-5}$ (°C)$^{-2}$ is an empirical parameter. In this case, we are talking about the behavior of water within the temperature range from 0 to 8°C, the inversion temperature in which is $T_i = 4$ °C.

In [2], the case of a given constant heat flux at the lower boundary was considered numerically by a finite-difference method. The critical Rayleigh numbers turned out to be smaller than those found from the linear theory.

The linear stability of the mechanical equilibrium of a layer with solid boundaries was investigated in [3–6]. It is shown that the problem of equilibrium stability of a fluid layer with density inversion under the condition of solid isothermal boundaries is mathematically equivalent to the problem of stability of the Couette flow between rotating cylinders. In this case, the ratio of the rotation speeds of the inner and outer cylinders plays a role similar to the role of the ratio of the depth of the stably stratified part of the layer to its total thickness. A simple algebraic formula is obtained that relates the Taylor number and the Rayleigh number. In [3], the cases of a fixed temperature and a fixed heat flux at the boundaries were considered. Theoretical and experimental studies of the influence of density inversion on the occurrence of convection in a horizontal water layer with solid isothermal boundaries were carried out in [4]. Both analytical and experimental results have shown that the presence of density inversion leads to stabilization of the layer equilibrium. In [5], the influence of the position of the density inversion point inside the layer on the critical value of the Rayleigh number and the intensity of supercritical convective flows with rectangular (projected onto a horizontal plane) cell shape

was studied numerically. To determine the conditions for the occurrence of convection in a horizontal water layer near the density extremum point, the equation of state $\rho = \rho_m \left(1 - \alpha |T - T_i|^\gamma\right)$ was used in [6], based on measurements of changes in the density of both pure and salt water. Water with different salinity corresponded to different values of parameters α and γ. It has been established that the effects associated with the presence of density inversion play a stabilizing role.

The stability of a water layer formed as a result of the melting of ice heated from above by a constant radiation flux (a heat flux is specified at the upper boundary) was examined in [7]. The lower boundary of the liquid layer had a melting point of 0°C. The temperature dependence of the density was assumed to be cubic. It has been theoretically and experimentally shown that the critical Rayleigh number depends on the free surface temperature T_2, if $T_2 < 8\,°C$, and does not depend on T_2 at $T_2 > 8\,°C$.

A linear analysis of the equilibrium stability was carried out in [8] taking into account the thermocapillary effect and thermal conditions of the third kind at the upper free boundary; the lower boundary was assumed to be solid and isothermal. The approximation of the temperature dependence of the density in the form of a cubic polynomial adopted in this work made it possible to consider the problem in a wider temperature range than with a quadratic dependence.

The influence of the finite thermal conductivity of arrays was investigated in [3]. An analysis of the case of two solid arrays showed that in the presence of a temperature inversion of the density, the final thermal conductivity of the arrays, as well as in the absence of inversion, leads to destabilization. The qualitative dependence of the critical Rayleigh number on the thickness of a stably stratified layer $R = 1 - z_i$ (to take into account the effect of density inversion, we used the dimensionless coordinate of the density inversion point z_i) did not depend on the boundary conditions. The combined effect of both the density maximum and the final thermal conductivity of the arrays, at large negative R ($z_i \gg 1$) led to destabilization of the Rayleigh number relative to the Boussinesq limit $\mathrm{Ra}_c = 1708$, and with an increase R (decrease z_i) its stabilization was observed.

In [9] subsequent calculations by the spectral method on the supercomputer at Moscow State University (Moscow) are aimed at studying the features of convection propagation with maximum approximation to horizontal layers of water located between free and non-deformable planes. The supercritical flow was assumed according to the regulations, and for the chosen periodicity of the manifestation of the two main branches of hysteresis, solutions were found that have a value of the characteristic scale. The transition to chaos through quasi-periodic regimes and intermittency is described.

The problem of water convection, the density of which depends quadratically on temperature and pressure, was considered in [10]. The limits of applicability for convection in Lake Baikal of the Veronis formula (1) are determined. For this purpose, the linearization method was used to study the nature of the equilibrium state of a horizontal water layer up to 1000 m thick with a free boundary with respect to small disturbances. It is found that the state of mechanical equilibrium of the water layer is unstable. Neutral curves are constructed and critical Rayleigh numbers are found. A comparison is made with the results of solving a similar problem for the limiting case when the density is determined by formula (1). It is shown that the applicability of the Veronis expression is limited to a layer depth of up to 150 m, while the average depth of Baikal is 750 m.

In [11], co-authored by the authors of this paper, it was revealed that in the only known paper [3] devoted to the analysis of convection in a horizontal liquid layer with free upper and solid lower boundaries and a prescribed heat flux at both boundaries, when deriving linearized equations for the amplitudes of perturbations, two terms are lost. As a result of solving the well-formulated problem of linear stability below, it is shown that the thermal conditions corresponding to a fixed heat flux contribute to the existence of long-wavelength perturbations. Long-wavelength perturbations are not always possible, but only for a sufficiently thick unstable stratified layer, namely, for $z_i > 5/9$ (here z_i is the thickness of the unstable stratified sublayer, which is dimensionless over the height of the entire layer). At $z_i > 0.61$, long-wavelength perturbations are the most dangerous. Cellular perturbations are the most dangerous in the region $z_i < 0.61$. The boundaries of stability are determined for both types of perturbations.

In [12], the form of critical perturbations was found in the formulation of [11]. Long-wave disturbances have the form of a plane-parallel flow consisting of two or more counter flows. The shape of cellular perturbations is an infinite set of identical cells with flat vertical boundaries. In the lower part of each cell, there is an intense vortex covering the region of unstable stratification and penetrating into the region of stable stratification. For sufficiently small values of z_i, one or several increasingly weaker vortices can form above this vortex.

The studies of instability and the structure of critical perturbations carried out in [11, 12] can be considered as the first steps in understanding a more global problem — establishing the structure and regimes of convection in elongated horizontal open rectangular cavities with different aspect ratios L (the ratio of the horizontal size to the height) for a given vertical heat flow on horizontal faces.

An analysis of the literature showed that in cavities filled with a liquid with a linear dependence of density on temperature, the characteristic long-wave nature of the instability, elucidated in the framework of the linear theory of stability for an infinite layer [13], that is $L = \infty$, for , is clearly manifested already in moderately elongated cavities: with $L = 4$, $L = 3$ and even $L = 2$ [14, 15]. In such cavities, the supercritical motion in a wide range of supercriticality has the form of one large-scale elongated vortex. As the L increases, critical Rayleigh number tends to the value determined by the methods of the linear stability theory for an infinite layer. In a significantly elongated cavity ($L = 5$), only the first supercritical motion is large-scale; further, as the supercriticality increases, it experiences a number of hysteresis transitions to the cellular form of convection.

Thus, the long-wavelength nature of the instability in a liquid without thermal density inversion takes place already in a moderately elongated cavity (with aspect ratio $L = 2$). In more elongated cavities, it is also present, but in a strongly elongated cavity ($L = 5$) it quickly becomes unstable, and the convection regime changes to cellular.
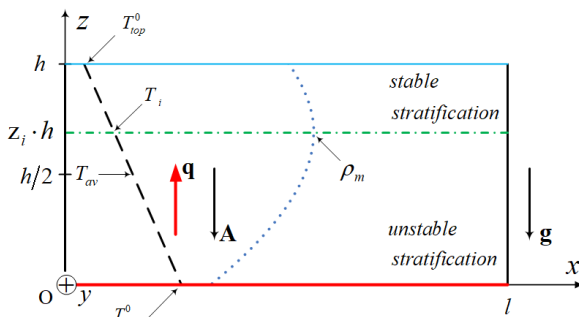
Fig. 1. Problem geometry; the equilibrium temperature distribution $T^0(z)$ is shown by a dashed line, and the density distribution $\rho^0(z)$ in the state of mechanical equilibrium is shown by a dotted line; dash-dotted line – the boundary between stable and unstable stratification.

An analysis of works [11, 12, 14, 15] suggests that the long-wavelength nature of the instability in a layer of melt water, i.e., in a liquid with density inversion, will be found in a moderately elongated cavity with aspect ratio $L = 2$.

Therefore, the purpose of this work is to study the stability of mechanical equilibrium and supercritical regimes of fluid convection with thermal density inversion in a horizontal cavity with an aspect ratio $L = 2$ for two characteristic values of the position of the inversion point $z_i = 0.5$ and $z_i = 0.75$ by a finite difference method. The choice of values z_i is due to the fact that at the first value in an infinite layer the nature of the instability is cellular, while at the second it is long-wavelength.

2. Formulation of the problem and solution method

Let us consider a horizontal rectangular cavity with height h and width l (Fig. **1**) filled with water and located in a uniform gravity field $\mathbf{g}$. A fixed vertical heat flux $\mathbf{q}$ is set on both horizontal boundaries $z = 0, h$, and the side boundaries $x = 0, l$ are thermally insulated. The dependence of density on temperature is assumed to be quadratic (1).

The rectangular right-handed Cartesian coordinate system $(Oxyz)$ is defined so that the axis Ox passes along the more heated horizontal boundary, and the axis Oz passes along the left thermally insulated vertical one. The upper bound is assumed to be free, and all other bounds are solid.

To describe the motion of a fluid, we apply the equations of free thermal convection of a fluid with temperature density inversion in the Boussinesq approximation [11]:

$$\frac{\partial \mathbf{v}}{\partial t} + \mathbf{v} \cdot \nabla \mathbf{v} = -\frac{1}{\rho_m} \nabla p + \nu \Delta \mathbf{v} - \alpha_2 \mathbf{g}(T - T_i)^2, \tag{2}$$

$$\frac{\partial T}{\partial t} + \mathbf{v} \cdot \nabla T = \chi \Delta T, \tag{3}$$

$$\operatorname{div} \mathbf{v} = 0. \tag{4}$$

Here, p is the addition to the hydrostatic pressure distribution in a stationary fluid. The coefficients of kinematic viscosity ν, and thermal diffusivity χ, are considered constant. The thermocapillary effect, the effects of evaporation and radiation at the upper free boundary are neglected. The estimates obtained in [10] show that under conditions of open water bodies (ponds, lakes), the Boussinesq approximation can be used for depths of the order of hundreds of meters.

Let's write the boundary conditions:
– on thermally insulated vertical walls

$$x = 0,\ l: \quad \mathbf{v} = 0, \quad \frac{\partial T}{\partial x} = 0 ; \tag{5}$$

– on the solid lower and free upper horizontal faces

$$z = 0: \quad \mathbf{v} = 0, \quad \frac{\partial T}{\partial z} = -A ; \tag{6}$$

$$z = h: \quad \mathbf{v}_z = 0, \quad \frac{\partial \mathbf{v}_x}{\partial z} = 0, \quad \frac{\partial \mathbf{v}_y}{\partial z} = 0, \quad \frac{\partial T}{\partial z} = -A . \tag{7}$$

From the conditions for temperature contained in (5)–(7) (a constant vertical temperature gradient is set on the horizontal boundaries of the cavity, and the side walls are thermally insulated), it follows that the amount of heat entering the cavity through the lower boundary per unit time is equal to the heat flux through the upper boundary. Therefore, the average temperature of the liquid in the layer T_{av} does not depend on the intensity of convection and is determined only by the initial temperature distribution in the liquid.

The problem (2)–(7) has a solution corresponding to the state of mechanical equilibrium:

$$\mathbf{v}^0 = 0, \tag{8}$$

$$T^0 = -Az + T_{av} + \frac{Ah}{2}, \tag{9}$$

$$p^0 = -\frac{1}{3}\alpha_2 g \rho_m A^3 h^3 \left(\frac{T_{av} + Ah/2 - T_i}{Ah} - \frac{z}{h} \right)^3 + \text{const} . \tag{10}$$

According to (9), in the state of mechanical equilibrium, the temperature at the horizontal boundaries is constant and is determined from the expressions:

$$T^0_{bottom} = T_{av} + \frac{Ah}{2}, \tag{11}$$

$$T^0_{top} = T_{av} - \frac{Ah}{2} . \tag{12}$$

We introduce the notation

$$z_i = \frac{T^0_{bottom} - T_i}{T^0_{bottom} - T^0_{top}} . \tag{13}$$

Substituting here (11), (12) we get:

$$z_i = \frac{T_{av} + Ah/2 - T_i}{Ah} . \tag{14}$$

From this, it can be seen that z_i is a dimensionless parameter and, depending on the ratio of the average liquid temperature and the inversion temperature, can take both positive and negative values.

Taking into account (14), expression (9) for the equilibrium temperature distribution will be rewritten in the form:

$$T^0 = T_i + Ah\left(z_i - z/h\right). \tag{15}$$

After substituting (15) into (1), we have the density distribution in the state of mechanical equilibrium:

$$\rho^0 = \rho_m\left(1 - \alpha_2 A^2 h^2\left(\frac{z}{h} - z_i\right)^2\right) \tag{16}$$

Differentiating this relation with respect to z, we obtain:

$$\frac{d\rho^0}{dz} = 2\rho_m\alpha_2 A^2 h\left(z/h - z_i\right) \tag{17}$$

As can be seen from formula (17), for $z_i \leq 0$ the entire layer $d\rho^0/dz < 0$, that is, in a fluid at rest, stable stratification is realized. At $0 < z_i < 1$, only the upper part of the layer is stably stratified $z_i h < z < h$, while the layer adjacent to the bottom of the cavity $0 < z < z_i h$ is stratified unstable (Fig. **1**). In this case, z_i the dimensionless thickness of the unstable stratified layer has a clear physical meaning and it is also the dimensionless coordinate of the boundary between the stably and unstable stratified layers. It also follows from (17) that for $z_i \geq 1$, the entire liquid layer is stratified unstable.

For the average temperature T_{av} and z_i the relation is fulfilled:

$$T_{av} - T_i = Ah\left(z_i - 1/2\right). \tag{18}$$

Thus, z_i, indicating the position of the inversion point in the equilibrium temperature distribution in the liquid, is connected by a simple formula with a positively determined average temperature of the liquid, which is a parameter of the problem. Therefore, z_i is also a problem parameter that takes both positive and negative values.

Let us introduce vector potentials into consideration:

$$\boldsymbol{\varphi} = \mathrm{rot}\,\mathbf{v}, \qquad \mathbf{v} = \mathrm{rot}\,\boldsymbol{\psi}. \tag{19}$$

We will assume that the supercritical flow is flat: the y-component of velocity is equal to zero and all variables do not depend on the y-coordinate. Therefore, the vector potentials $\boldsymbol{\varphi}$ and $\boldsymbol{\psi}$ will have non zero only y-components, which in the plane case have the meaning of vorticity and stream function:

$$\boldsymbol{\varphi} = \left(0, \varphi, 0\right), \qquad \boldsymbol{\psi} = \left(0, \psi, 0\right) \tag{20}$$

Let us also introduce into the analysis the temperature deviation from the inversion temperature:

$$\tilde{T} = T - T_i. \tag{21}$$

Then, after performing the operation with respect to (2) and using (19)–(20), one can obtain a system of equations for thermal convection in variables $\psi, \varphi, \tilde{T}$:

$$\frac{\partial\varphi}{\partial t} + \frac{\partial\psi}{\partial x}\frac{\partial\varphi}{\partial z} - \frac{\partial\psi}{\partial z}\frac{\partial\varphi}{\partial x} = \Delta\varphi - \mathrm{Gr}\,\tilde{T}\frac{\partial\tilde{T}}{\partial x}, \tag{22}$$

$$\frac{\partial\tilde{T}}{\partial t} + \frac{\partial\psi}{\partial x}\frac{\partial\tilde{T}}{\partial z} - \frac{\partial\psi}{\partial z}\frac{\partial\tilde{T}}{\partial x} = \frac{1}{\mathrm{Pr}}\Delta\tilde{T}, \tag{23}$$

$$\Delta \psi + \varphi = 0. \tag{24}$$

The tilde sign at $\tilde{T}$ is further omitted.

Equations (22)–(24) are written in dimensionless form. For this, the following units of measurement are introduced: for time h^2/v, for distance h, for temperature Ah, for velocity v/h, for stream function v and for vorticity v/h^2, as well as dimensionless complexes: $\mathrm{Pr} = v/\chi$ is the Prandtl number; similarity criterion Gr, which is an analogue of the Grashof number and is defined through the physical constants of the problem as

$$\mathrm{Gr} = \frac{2g\alpha_2 A^2 h^5}{v^2}. \tag{25}$$

We also introduce into consideration an analogue of the Rayleigh number Ra associated with Gr and Pr by the relation:

$$\mathrm{Ra} = \mathrm{Gr} \cdot \mathrm{Pr} = \frac{2g\alpha_2 A^2 h^5}{v\chi}. \tag{26}$$

We express the velocity components in terms of the current function:

$$\mathrm{v}_x = -\frac{\partial \psi}{\partial z}, \qquad \mathrm{v}_z = \frac{\partial \psi}{\partial x} \tag{27}$$

Then the conditions on the rigid lower and free upper horizontal boundaries take the form:

$$z = 0: \quad \psi = \frac{\partial \psi}{\partial z} = 0, \quad \frac{\partial T}{\partial z} = -1,$$
$$z = 1: \quad \psi = \varphi = 0, \quad \frac{\partial T}{\partial z} = -1, \tag{28}$$

and the boundary conditions on the solid side boundaries in the new variables (in dimensionless form) will be as follows:

$$x = 0: \quad \psi = \frac{\partial \psi}{\partial x} = 0, \quad \frac{\partial T}{\partial x} = 0,$$
$$x = L: \quad \psi = \frac{\partial \psi}{\partial x} = 0, \quad \frac{\partial T}{\partial x} = 0. \tag{29}$$

Here $L = l/h$ is the aspect ratio.

The state of mechanical equilibrium, when the fluid is at rest, is described in new variables and dimensionless form by the equations:

$$\psi^0 = \varphi^0 = 0, \quad T^0 = z_i - z. \tag{30}$$

The expression (18), relating the average temperature of the liquid with the coordinate of the inversion point at rest, in dimensionless variables will be rewritten in the form:

$$T_{ov} = z_i - 1/2. \tag{31}$$

Thus, the solution to problem (22)–(29) is determined by the Prandtl number Pr, Grashof number Gr, the coordinate of the inversion point z_i (or the average fluid temperature in the cavity), and the aspect ratio L.

The problem (22)–(29) was solved numerically by the finite difference method, all spatial derivatives were approximated by central differences on a uniform grid. The grid step was assumed to be $h = 1/64$. The aspect ratio in the calculations presented below was equal to two ($L = 2$). When approximating in time, an explicit scheme with a constant time step $h^2/10$ was used.

The Poisson equation (24) for the stream function was solved by the successive overrelaxation method. The boundary condition for the vorticity on the bottom and side solid walls was obtained using the Thom formulas [16]. The method used is described in more detail in [17].

3. Calculation results

Before performing the main calculations, in accordance with the above method, the formulated model and the difference method were verified. To do this, the critical Grashof number was calculated based on the well-studied problem of plane convection in a square cavity (that is, with an aspect ratio $L = 1$) with isothermal horizontal and thermally insulated vertical walls in the absence of density inversion. The critical Grashof number was found by extrapolating the linear dependence of the square of the stream function on the Grashof numbers obtained in calculations on a square grid with a step $h = 1/64$ towards lower values and then compared with the generally accepted value calculated by the methods of the linear theory of stability. This is how the critical Grashof number $\mathrm{Gr}_{cr} = 255$ was established.

It is known that for the case of thermally insulated side walls in a square cavity, the critical Rayleigh number rounded to four significant figures is $\mathrm{Ra}_{cr} = 2585$ [18], and the corresponding critical Grashof number at $\mathrm{Pr} = 10$, is 258.5. Thus, as a result of the verification analysis, it turned out that the calculated critical Grashof number differs from that determined with a high degree of accuracy by the methods of the linear theory of stability by less than 1.5%, which indicates the satisfactory accuracy of the used model and the numerical method of solution.

The main calculations were carried out for a cavity with an aspect ratio $L = 2$ at two values of the position of the inversion point: $z_i = 0.5$ and 0.75. The Prandtl number was assumed to be $\mathrm{Pr} = 10$. Based on the calculation results, for each of the given values z_i, the critical Grashof number was found in the region and the nonlinear supercritical convection regime was studied at a supercriticality reaching several tens.

3.1. Equal thickness of stably and unstable stratified sublayers

With equal layer thicknesses ($z_i = 0.5$) in the state of mechanical equilibrium, the lower liquid layer ($0 \le z \le 0.5$) is stratified unstable. On top of it is a stably stratified layer of a liquid. For a cavity infinitely extended in the horizontal direction ($L = \infty$), the state of the rest of the liquid (24) becomes unstable with respect to small normal perturbations when the Rayleigh number exceeds a critical value $\mathrm{Ra}_{cr}(\infty; 0.5) = 2.32 \cdot 10^4$ [11]. Hence it follows that the critical Grashof number for an infinitely elongated cavity and the value of the Prandtl number $\mathrm{Pr} = 10$ adopted in this work is equal to $\mathrm{Gr}_{cr}(\infty; 0.5) = \mathrm{Ra}_{cr}(\infty; 0.5)/\mathrm{Pr} = 2.32 \cdot 10^3$.

Let us consider the effect of a gradual increase in the Grashof number on the stability of mechanical equilibrium. The finite horizontal size of the cavity, due to the presence of solid vertical walls that slow down the development of perturbations, leads, as a rule, to an increase in the critical numbers for the occurrence of convective instability [13]. Therefore, the first series of calculations was carried out for the Grashof number $\mathrm{Gr} = 3000$ in the hope that it will exceed the critical, yet unknown, number $\mathrm{Gr}_{cr}(2; 0.5)$ for $L = 2$. The following distributions were set as the initial state:

$$\psi^0_{i,k} = 0, \qquad T^0_{i,k} = 0.5 - h \cdot k, \qquad \varphi^0_{i,k} = \varphi^c \qquad (32)$$

The initial value of the vorticity φ^c at all nodes of the grid was assumed to be 10. At lower absolute values of φ^c, for example, at $\varphi^c = 1$, the calculations show that the perturbation decays (32) and the equilibrium state of rest (30) is established.

Figure 2a shows the stationary supercritical solution obtained as a result of a numerical calculation of the evolution of the initial state (32) with $\varphi_c = 10$. The vortex structure of the supercritical flow corresponds to

the structure predicted by the linear theory [11, 12] for an infinite layer, i.e., it has a two-tier vertical shape, with intense eddies penetrating from the lower unstable stratified layer into the upper, stably stratified layer. The nonlinearity leads to curvature of the boundary between the tiers, it becomes wavy. A similar structure of supercritical flows was observed for isothermal boundaries in [2], as well as in [19, 20] when studying the convection of a vapor-gas mixture, which, like melt water, has an anomalous dependence of density on temperature.

In subsequent calculations, when solving with other values of the Grashof number, the method of continuation with respect to the parameter was used. The stationary state found earlier for a certain Grashof number Gr_1 was taken as the initial state, then the Grashof number was simultaneously changed by a step ΔGr, and by numerically solving the problem with this state, a new stationary state was obtained for the Grashof number $Gr_2 = Gr_1 + \Delta Gr$. The step size according to the Grashof number ΔGr varied from $\Delta Gr = 10$ to $\Delta Gr = 500$. Calculations have shown that such a stepwise increase in the value of the Grashof number from $Gr = 3000$ to $Gr = 14500$ leads to a smooth change in the structure of the supercritical flow. In each of the convective cells, the centers of intense vortices of the lower (stratified unstable) tier move towards the solid wall, and in each of the convective cells, the vortices are separated from the lower solid wall, in each cell a weak vortex is formed, opposite to the main one (Fig. **2***b*). The total number of large eddies becomes six. There is a strict separation of the flow by a vertical flat boundary into two equal cells (regime I).

A further increase in the Grashof number causes a bifurcation, which consists in doubling the number of convective cells along the horizontal coordinate (Fig. **2***b*). Such a steady state is achieved by increasing the last value of the Grashof number ($Gr = 14500$) from regime I by $\Delta Gr = 200$. The formation of a stationary vortex structure (regime II), shown in Figure **2***c*, is observed. The intensity of the convective flow in cells adjacent to solid vertical walls is noticeably weaker. A further increase in the Grashof number leads to the equalization of the intensities of neighboring vortices both in the lower and upper tiers (Fig. **2***d*). Figure **2***d* shows the stationary state for $Gr = 20000$. As the Grashof number decreases (at $Gr = 13000$), there is a transition to the previous regime I with two equal cells. The transition between regimes from I to II and vice versa is carried out in a hysteretic manner.
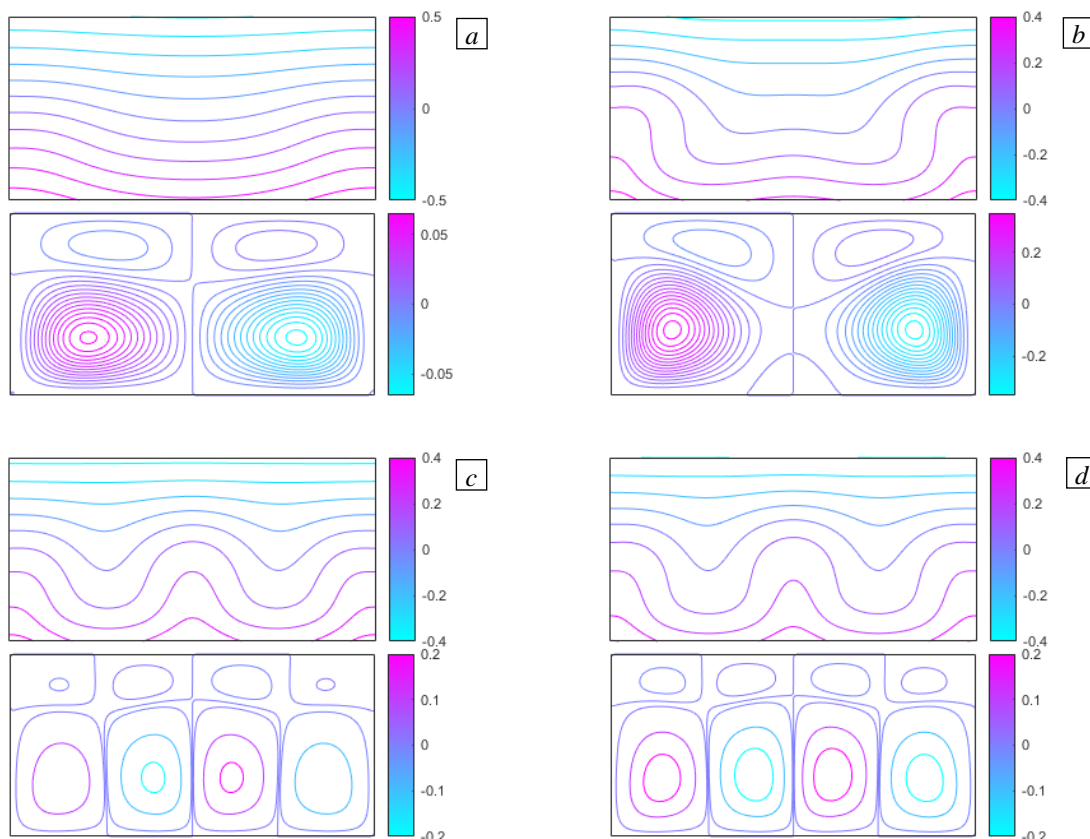
Fig. 2. Isotherms and streamlines of regimes I (*a*, *b*) and II (*c*, *d*) of supercritical convective flow at $z_i = 0,5$ for various values of the Grashof number; regime I: $Gr = 3000$ (*a*), $Gr = 14500$ (*b*); regime II: $Gr = 14700$ (*c*), $Gr = 20000$ (*d*).

To quantitatively characterize the change in the intensity of supercritical motions with an increase in the Grashof number, we use the Gr dependence on the maximum modulo value of the stream function in the cavity $\psi_m(\mathrm{Gr})$, and the specific kinetic energy of the convective motion $E(\mathrm{Gr})$, determined from the expression:

$$E(\mathrm{Gr}) = \frac{1}{2L}\int_0^1\int_0^L v^2 \, dz \, dx = \frac{1}{2L}\int_0^1\int_0^L \psi\varphi \, dz \, dx. \tag{33}$$

The calculated dependences $\psi_m(\mathrm{Gr})$ and $E(\mathrm{Gr})$ for the range of Grashof numbers $0 \leq \mathrm{Gr} \leq 20000$ are shown in Figure 3. At the Grashof numbers $2600 \leq \mathrm{Gr} \leq 10000$, the kinetic energy of stationary solutions depends linearly on the Grashof number (dependence by the least squares method):

$$E = 2.66\cdot 10^{-5}\cdot(\mathrm{Gr} - 2.56\cdot 10^3) \tag{34}$$

Extrapolating this dependence to zero, we obtain the critical value of the Grashof number $\mathrm{Gr}_{cr}(2;0.5) = 2.56\cdot 10^3$. Calculations near this value showed that at $\mathrm{Gr} = 2500$ a small initial perturbation decays, and at $\mathrm{Gr} = 2600$, it grows up to the moment when a stationary regime begins to establish, similar to that shown in Fig. 2a. Given that in the test calculations described above with a known value of the critical Grashof number, the method used showed an accuracy of at least 1.5%, we can conclude that the extrapolated value of the critical Grashof number will differ from the true value by less than 2%. In the same range of Grashof numbers ($2600 \leq \mathrm{Gr} \leq 10000$), the root law holds for the maximum modulo value of the current function:

$$\psi_m = 3.46\cdot 10^{-3}\cdot\sqrt{\mathrm{Gr} - 2.56\cdot 10^3}. \tag{35}$$

Dependencies (34) and (35) are shown in Figure 3 by dashed lines.
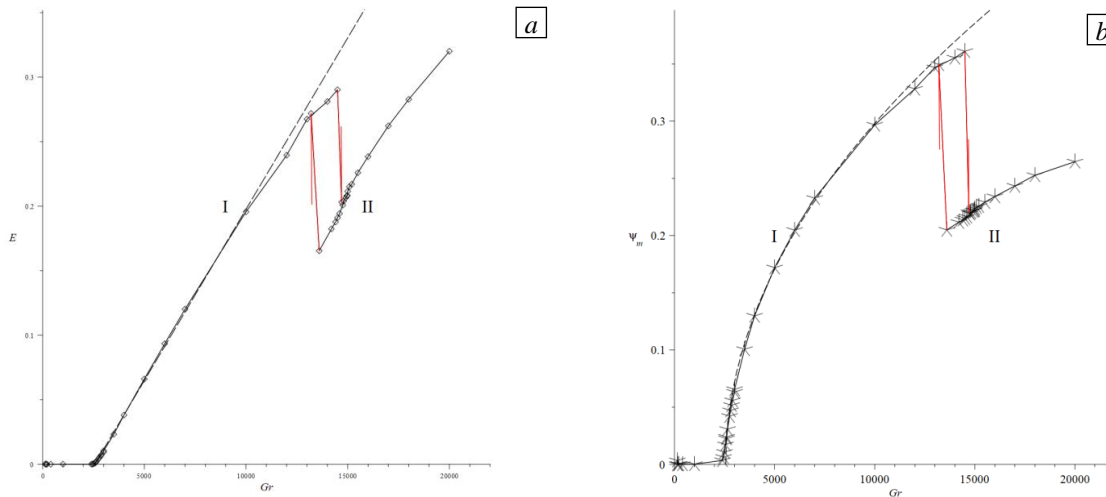
Fig. 3. Dependences of the kinetic energy (*a*) and the maximum stream function (*b*) in regimes I and II of stationary supercritical convective motion in the cavity for the case $z_i = 0.5$.

A verification calculation on a finite-difference grid of square cells with a step $h = 1/128$ for the value of the Grashof number $\mathrm{Gr} = 20000$ showed that the flow pattern to the details corresponds to that shown below in Figure 4*d*, and the value of the kinetic energy differs from that obtained on a grid with a step $h = 1/64$ of less than 0.07%.

3.2. A thin stably stratified sublayer over a thick unstable stratified sublayer

Let us consider the case when the state of mechanical equilibrium is realized in the cavity with the lower layer consisting of three-quarters of the liquid in the cavity ($0 \leq z \leq 0.75$), stratified unstable, and on top of it

there is a layer that is three times thinner and stably stratified. With an infinite length of the cavity in the horizontal direction ($L = \infty$), the state of the rest of the liquid (24) at $z_i > 0.61$ becomes unstable with respect to long-wave perturbations when the Rayleigh number exceeds its critical value, determined by the formula [11]:

$$\text{Ra}_{cr}(\infty; z_i) = \frac{320}{z_i - 5/9}. \tag{36}$$

From (36) it follows that the critical Grashof number for an infinitely elongated cavity and the value of the Prandtl number $\text{Pr} = 10$ adopted in this work is: $\text{Gr}_{cr}(\infty; 0.75) = 165$. As a rule, the finite horizontal size of the layer leads to an increase in the critical value of the Grashof number. Therefore, the first series of calculations was carried out for the Grashof number $\text{Gr} = 300$ in the hope that it will exceed the critical (still unknown) number $\text{Gr}_{cr}(2; 0.75)$. As in the case $z_i = 0.5$ considered above, as the initial state we set distributions (32) with a controlled initial perturbation φ^c. Figure 4a shows the stationary solution obtained as a result of a numerical calculation of the evolution of the initial state (26) for the specified Grashof number with the initial perturbation $\varphi^c = 10$. Calculations at significantly lower absolute values of φ^c, for example, at $\varphi^c = 1$, led to damping of the perturbed state (26). As can be seen from the figure, the supercritical flow is single-vortex and fills the entire cavity, which indicates the long-wavelength nature of the instability.
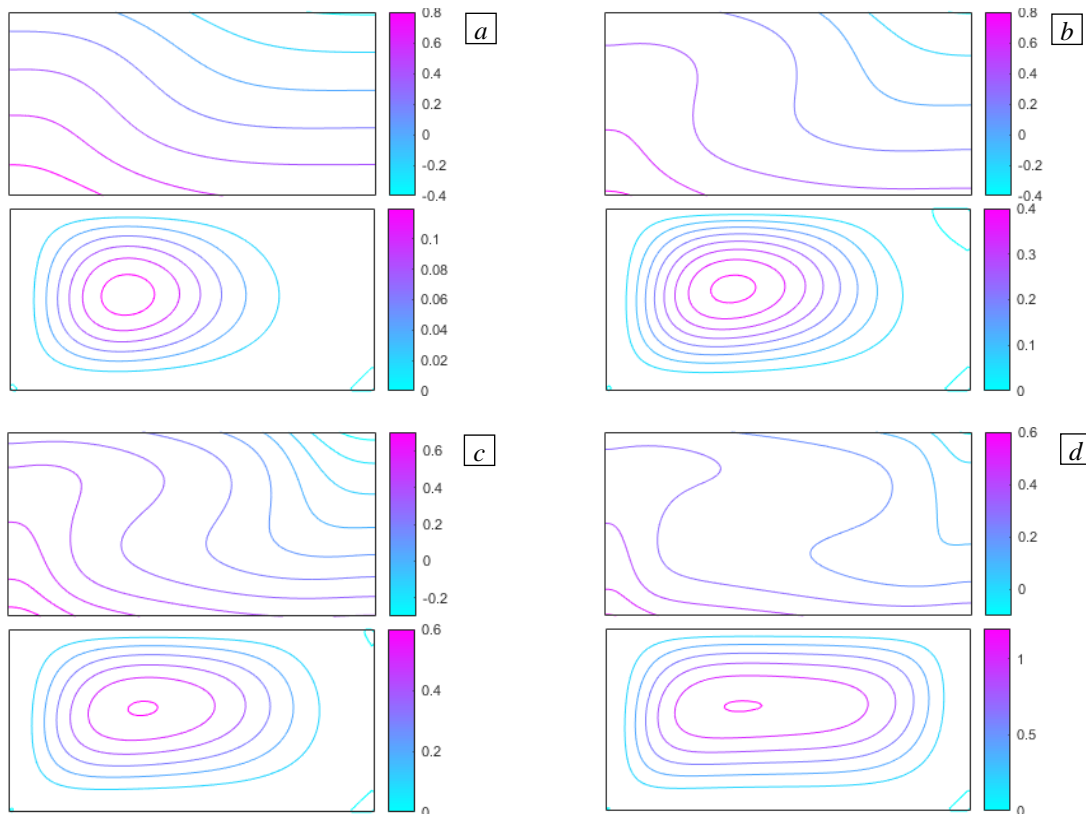
Fig. 4. Isotherms (upper rectangle) and streamlines (lower rectangle) of the supercritical convective flow at $z_i = 0.75$ for different values of the Grashof number: 300 (a), 1000 (b), 2000 (c), 20000 (d).

Calculations have shown that a stepwise increase in the Grashof number from $\text{Gr} = 300$ to $\text{Gr} = 20000$ does not lead to a qualitative change in the structure of the supercritical flow. It remains single-vortex, which confirms its long-wave nature (see Fig. 4b-d). The asymmetry of the flow is due to the beginning of the formation of an upward flow in the convective boundary layer near the left vertical wall, as a result, the center of the vortex is displaced. The dependences $\psi_m(\text{Gr})$ and $E(\text{Gr})$ obtained in the least squares calculations for the range of the Grashof numbers $0 \leq \text{Gr} \leq 10000$ are shown in Figure 5. In the region of the Grashof numbers $250 \leq \text{Gr} \leq 2500$, the kinetic energy of stationary solutions depends linearly on the Grashof number:

$$E = 2.96 \cdot 10^{-4} \cdot (\text{Gr} - 2.30 \cdot 10^2). \tag{37}$$
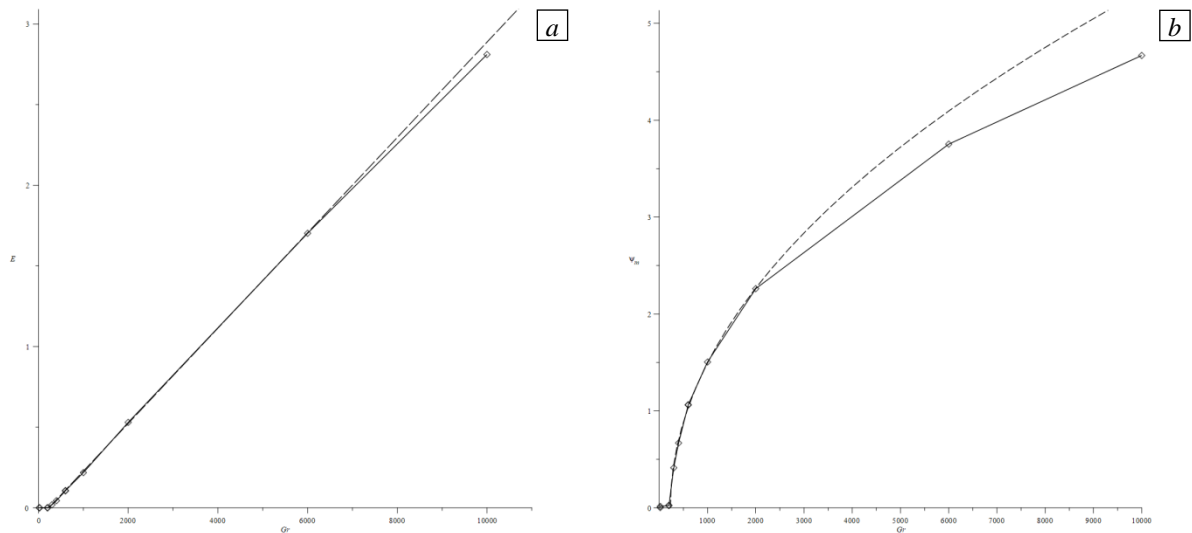
Fig. 5. Dependences of the kinetic energy (*a*) and the maximum stream function (*b*) of stationary supercritical convective motion in the cavity for the case $z_i = 0.75$.

Extrapolating dependence (37) to zero, we find the critical value of the Grashof number $\mathrm{Gr}_{cr}(2; 0.75) = 2.30 \cdot 10^2$. Calculations near this value showed that the initial small perturbation attenuates for $\mathrm{Gr} = 200$, and for $\mathrm{Gr} = 250$ increases until the establishment of the stationary regime shown in Fig. **4***a* for $\mathrm{Gr} = 300$. Taking into account the above accuracy of test calculations of the problem for conditions with a known value of the critical Grashof number, it can be assumed that the extrapolated value of the critical Grashof number differs from the true value by less than 2%. In the same range of the Grashof numbers, the root law holds for the maximum current function in absolute value:

$$\psi_m = 1.46 \cdot 10^{-2} \cdot \sqrt{\mathrm{Gr} - 2.30 \cdot 10^2}. \tag{38}$$

A verification calculation on a square grid with a step $h = 1/128$ for the value of the Grashof number $\mathrm{Gr} = 20000$ showed that the flow pattern to the details corresponds to that shown in Figure **4***d*, and the maximum value of the kinetic energy differs from that obtained on a grid with a step $h = 1/64$ of less than 0.04%.

4. Conclusion

Calculations have shown that in a moderately elongated horizontal cavity with an aspect ratio $L = 2$ for the case $z_i = 0.5$ when the thickness of the unstable stratified layer z_i is equal to the thickness of the stably stratified layer $1 - z_i$, the supercritical flow demonstrates a two-cell structure along the horizontal coordinate. The vertical structure of the cells has a complex two-tier character, which changes with increasing heating intensity. At $z_i = 0.75$, the structure of the supercritical flow is simple, single-vortex, smoothly deforming with increasing heating intensity.

At equal thicknesses of stably and unstable stratified layers ($z_i = 0.5$), the two-cell supercritical flow in the region of approximately six-fold supercriticality passes in a hysteretic manner into a four-cell flow. When the thickness of the stably stratified layer $1 - z_i$ is three times less than the thickness of the unstable stratified layer $z_i = 0.75$, the supercritical convective flow as a whole takes the form of a horizontally elongated single-vortex cell. As the Grashof number increases to a value corresponding to about a hundredfold supercriticality, the flow remains single-vortex and does not experience bifurcations.

Note that with an increase in the intensity of heat transfer through the layer in the central region of the cavity near the surface and bottom, a pronounced plane-parallel flow is formed (see Fig. **4***d*). Therefore, in the future, it is necessary to evaluate the stability of this plane-parallel flow with respect to plane cellular perturbations.

Calculations have shown that at Grashof numbers exceeding 20000 by 10–20%, oscillatory convection modes arise, for the consideration and classification of which it is planned to conduct additional studies, in which the thermocapillary effect at the free boundary is supposed to be taken into account. Possibly, it can lead to the emergence of a new mechanism of cellular instability.

References

1. Veronis G.Penetrative convection // Astrophys.J.,–1963, V.137, № 2.– pp.641–663.

2. Moore D.R, Weiss N.O. Nonlinear penetrative convection // J. Fluid Mech. 1973. V. 61. № 3. P. 553– 581. https://doi.org/10.1017/S0022112073000868.

3. Merker G.P., Waas P., Straub J., Grigull U. Einsetzen der Konvektion in einer von unten gekuben Wasserschicht bei Temperaturen unter 4^0 C // Warme und Stoffubertrag. 1976. V. 9. № 2. P. 99 – 110. https://doi.org/10.1007/BF01589463.

4. Hawng L.-T., Lu W.-F., Mollendorf J.C. The effects of the density extremum and boundary conditions on the stability of a horizontally confined water layer // Int. J. Heat Mass Transfer. 1984. V. 27. № 4. P. 497 – 510. https://doi.org/10.1016/0017-9310(84)90023-1.

5. Nadolin K.A. Convection in a horizontal fluid layer with specific-volume inversion. Fluid Dyn., 1989, vol. 24, pp. 35-41.https://doi.org/10.1007/BF01051475.

6. Mollendorf J.C., Jann K.H. Onset of Convection in a Horizontal Layer of Cold Water J. Heat Transfer. 1983. V. 105, №3, P.460-465. https://doi.org/10.1115/1.3245607.

7. Seki N., Fukusako S., Sugawara M.A. Criterion of Onset of Free Convection in a Horizontal Melted Water Layer with Free Surface // J. Heat Transfer. 1977. V. 99, № 1, P. 92-98. https://doi.org/10.1115/1.3450661.

8. Wu R.-S., Cheng K.C. Maximum density effects on thermal instability induced by combined buoyancy and surface tension // Int. J. Heat and Mass Transfer. 1976. V. 19. № 5. P. 559 – 565. https://doi.org/10.1016/0017-9310(76)90170-8.

9. Kuznetsova D. V., Sibgatullin I. N.Transitional regimes of penetrative convection in a plane layer *//Fluid Dynamics Research.* 2012.Vol. 44, №. 3. – P. 031410.doi: 10.1088/0169-5983/44/3/03`410.

10. Bekezhanova V. B. Stability of the equilibrium state in a convection model with nonlinear temperature and pressure dependences of density //*Journal of Applied Mechanics and Technical Physics*. – 2007. – Vol. 48. – No. 2. – P. 200-207. https://doi.org/10.1007/s10808-007-0026-7

11. Lyubimov *D.V., Lyubimova T. P., Sharifulin V. A.* Onset of Convection in a Horizontal Fluid Layer in the Presence of Density Inversion under Given Heat Fluxes at Its Boundaries//*Fluid Dynamics,* 2012. Vol. 47, № 4, P. 448–453. https://doi.org/10.1134/S0015462812040035

12. Sharifulin V.A., Lyubimova T. P. Structure of critical perturbations in a horizontal layer of melted water with the prescribed heat flux at the boundaries //*IOP Conf. Series: Mater. Sci. and Eng.* – IOP Publishing, 2017. – V. 208. – №. 1. – P. 012025.doi:10.1088/1757-899X/208/1/012025.

13. Gershuni G. Z., Zhukhovitskii E. M. *Convective stability of incompressible fluids.* Israel Program for Scientific Translations, 1976. 337 p.

14. Sharifulin V.A., LyubimovaT.P.Supercritical Convection of Water in an Elongated Cavity at a Given Vertical Heat Flux//*J. Sib. Fed. Univ. Math. Phys.* 2021.Vol. 14, №2.P. 186–194. doi: 10.17516/1997-1397-2021-14-2-186-194.

15. Sharifulin V.A., Lyubimova T.P. A hysteresis of supercritical water convection in an open elongated cavity at a fixed vertical heat flux //*Microgr. Sci. and Tech.*2021. Vol. 33. №. 3. P. 1-9. https://doi.org/10.1007/s12217-021-09887-3.

16. Thom A., Apelt C.J. *Field computations in engineering and physics.*– Van Nostrand, 1961.

17. Sharifulin A. N., Poludnitsin A. N. The borders of existence of anomalous convection flow in the inclined square cylinder: Numerical determination //*St. Petersburg Polytech. Univ. J.: Phys. and Math.* – 2016. – V. 2. – №. 2. – P. 150-156.

http://dx.doi.org/10.1016/j.spjpm.2016.05.013.

18. Mizushima J. Onset of the thermal convection in a finite two-dimensional box//J. Physical Society of Japan. 1995. Vol. 64. №. 7.P. 2420–2432. . https://doi.org/10.1143/JPSJ.64.2420

19. Palymskiy I. B. et al. Rayleigh–Benard convection in a gas-vapor medium at the temperature close to the critical tempera-ture //*Journal of Physics: Conference Series.* – IOP Publishing, 2019. – V. 1382. – №. 1. – P. 012200.doi:10.1088/1742-6596/1382/1/012200.

20. Zhang L. et al. Rayleigh-Bénard convection of a gas-vapor mixture with abnormal dependence of thermal expansion coefficient on temperature //*International Communications in Heat and Mass Transfer.* – 2021. – V. 124. – P. 105245. https://doi.org/10.1016/j.icheatmasstransfer.2021.105245